Academic Journal of Chemistry
ISSN(e): 2519-7045, ISSN(p): 2521-0211
Vol. 8, Issue. 3, pp: 45-55, 2023
URL: https://arpgweb.com/journal/journal/20
DOI: https://doi.org/10.32861/ajc.83.45.55

Academic Research Publishing Group

Original Research **Open Access**

Experimental (NMR) and Theoretical (DFT Method) Studies of the Nucleophilic Substitution Reaction of 1-Methyl-4-, 6- and 7-NitroIndazoles by 2-(p-Tolyl) Acetonitrile

Assoman Kouakou
Laboratoire des Sciences et Technologies de l'Environnement Université Jean Lorougnon Guédé, Daloa, Côte d'Ivoire

Mougo André Tigori (Corresponding Author)
Laboratoire des Sciences et Technologies de l'Environnement Université Jean Lorougnon Guédé, Daloa, Côte d'Ivoire
Email: tigori20@yahoo.fr

Cissé M'Bouillé
Laboratoire des Sciences et Technologies de l'Environnement Université Jean Lorougnon Guédé, Daloa, Côte d'Ivoire

Sylla Tahiri
Laboratoire des Sciences et Technologies de l'Environnement Université Jean Lorougnon Guédé, Daloa, Côte d'Ivoire

Coulibaly Bakary
Groupe Enval laboratoire, Abidjan, Côte d'Ivoire

El Mostapha Rakib
Ecole Supérieur de Technologie Université Sultan Moulay Slimane, Fkih Ben Salah, Maroc

Article History
Received: 14 July, 2023
Revised: 25 September, 2023
Accepted: 5 October, 2023
Published: 7 October, 2023

Abstract

Theoretical and experimental study of the reactivity between alkyl nitroindazole molecules and aryl acetonitrile molecules was evaluated by Density Functional Theory (DFT) using a basis set of B3LYP/6-311G (d, p) level and experimental Nuclear Magnetic Resonance (NMR) data. Global quantum chemical parameters derived from DFT showed that these compounds are reactive while NMR data indicated the influence of nitro group on ortho, meta and para positions. The distinction atoms capable of undergoing nucleophilic and electrophilic attacks at the level of each molecule were spread by Fukui functions and dual descriptor. This distinction has helped to explain the mechanism of some nitro derivatives formation. Experimental and theoretical results are convergent and consistent.

Keywords: Alkyl nitroindazole; Aryl acetonitrile; Density functional theory; Nuclear magnetic resonance.

1. Introduction

Substituted heterocyclic compounds can offer a high degree of structural diversity and have been found to be widely useful as therapeutic agents. Among various heterocyclic structures, indazole derivatives have been widely used in medicinal chemistry [1] and drug discovery [2]. They exhibit a wide range of biological activities, including HIV protease inhibition [3], anti-inflammatory [4], antimicrobial [5], antispermatogenic [6], antiplatelet [7], and anticancer [8].

Research work on substituted heterocyclic molecules is widely multiplied both through purely chemical (synthesis) [9] and physical (reactivity) [10] studies. However, very little research has been devoted to indazole derivatives.

Among these works, Assoman et *al* reported in 2015 [11], a detailed spectroscopic and electrochemical study on N-alkylated derivatives of 4-, 5-, 6- and 7-nitroindazoles. This study permits to have a clear representation of electronic distribution for the studied molecules, useful for understanding and orienting indazole nucleus reactivity.

In 2020, the same authors developed new poly-substituted indazoles with good antiproliferative activities: 2-(aryl)-2-(7(4)-(arylsulphonyl)-oxime-1-alkyl-1H-indazol-7 (4)-ylidenes and 8-(4-Chlorophenyl)-1-methyl-1H-isoxazolo[3,4-g]indazole from the aromatic nucleophilic substitution of 1-alkyl-4(6)(7)- nitroindazoles by aryl-acetonitriles [12].

This study clearly underlines the correlation between indazole structure and its reactivity.

The originality of this study motivates our interest in understanding the true reasons for the chemical and physical reactivity of the indazole nucleus. This reactivity is often explained by quantum chemistry. In fact quantum chemistry studies also assist in reducing experimental costs involved in testing numerous compounds, in order to synthesize those with the best reactivity [13]. With this in mind, Density Functional Theory (DFT) is increasingly used to predict the geometric and electronic properties of compounds likely to be used in pharmaceutical, household and industrial applications [14, 15]. In order to support NMR data analysis, a theoretical study based on DFT has

been requested. Interpretation of Global and local quantum chemical parameters derived from this theory helps to understand and explain the electronic distribution within these compounds. In addition, this theory applies to a variety of organic molecules and provides reliable results that are consistent with experimental data [16-18]. For this study, DFT calculations are performed to establish a link between the molecular structure of indazole derivatives and their reactivities. These calculations, performed in the gas phase, allowed global and local reactivity parameters determination.

The aim of this work is to carry out a theoretical (DFT) and experimental study of the reactivity between alkyl nitroindazole molecules and aryl acetonitrile molecules. Therefore, in this study, it is necessary to establish a correlation between the global reactivity parameters and the experimental NMR data of the studied molecules. In addition, the identification of atoms susceptible to nucleophilic and electrophilic attack within each compound will be proven.

2. Material and Method

2.1. Studied Molecules

The molecular structures of the various molecules involved in this study are shown in Figure 1.

Figure-1. Different molecules studied

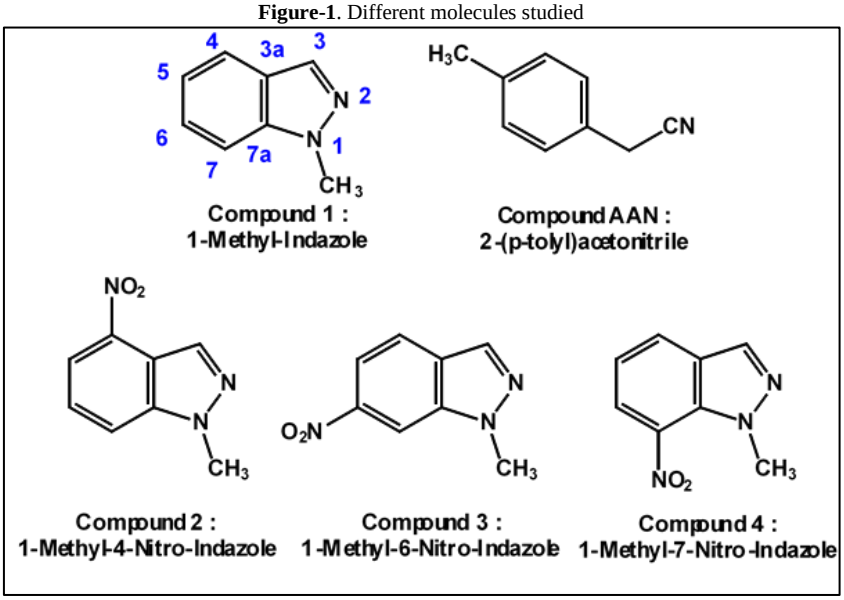

2.2. Spectroscopic Studies

Spectroscopic analysis of compounds was performed at the Department of Industrial Chemistry Toso Montanari Alma Mater Studiorum University of Bologna, Italy [2-4]. NMR data of 1-meyhyl-Indazole are from the literature.

^{1}H and ^{13}C NMR spectra were recorded at 600 MHz and 150.82 MHz (Bruke), respectively, in chloroform ($CDCl_3$) and dimethyl sulfoxide (DMSO). Chemical shifts are reported in δ (ppm) relative to $CDCl_3$ solvent (7.26 and 77.0 ppm for ^{1}H and ^{13}C NMR spectra, respectively). Coupling constants are reported in Hertz (Hz). ^{13}C NMR signal multiplicities were assigned by the distortion-free polarisation transfer enhancement (DEPT) method and, in some cases, by single heteronuclear quantum coherence gradient (g-HSQC) and/or multi-bond heteronuclear correlation gradient (HMBC) analysis.

2.3. Quantum Chemical Calculations Details

In the present investigation, a computer modeling technique based on DFT calculations were performed by gaussian 09 software [19]. These calculations were carried by hybrid functional B3LYP [20, 21], using 6-311G (d, p) basis set. This basic set was used to explore the relationship between electronic structure of studied compounds and their ability to react with other molecules. Each compound optimization geometry was performed using a computer graphics application: GaussView 5.0. Thus the optimized structure of each molecule is shown in Figure 2. The numerous relevant global chemical variables resulting from this technique were determined they are: highest occupied molecular orbital energy (E_{HOMO}), lowest unoccupied molecular orbital energy (E_{LUMO}), Energy gap (ΔE), electronegativity (χ), hardness (η), softness (σ) and electrophilicity index (ω) and total energy (E_T). These parameters are expressed according to the following equations [22, 23]:

$$\Delta E = E_{\mathrm{LUMO}} - E_{HO\mathrm{MO}} \quad (1)$$

$$I = -E_{HO\mathrm{MO}} \quad (2)$$

$$A = -E_{\mathrm{LUMO}} \quad (3)$$

$$\chi = -\mu_p = \left(\frac{\partial E}{\partial N}\right)_{v(r)} \quad (4)$$

$$\chi = \frac{I+A}{2} = -\frac{E_{LUMO}+E_{HOMO}}{2} \quad (5)$$

$$\eta = \frac{I-A}{2} = \frac{E_{LUMO}-E_{HOMO}}{2} \quad (6)$$

$$\sigma = \frac{1}{\eta} = \frac{2}{I-A} \quad (7)$$

$$\omega = \frac{\mu_P^2}{2\eta} = \frac{(\mathrm{I+A})^2}{4(\mathrm{I-A})} \quad (8)$$

The local reactivity parameters based on Fukui and dual descriptor functions were determined by the following equations [24-26]:

$$f_k^+ = q_k(N+1) - q_k(N) \quad (9)$$

$$f_k^- = q_k(N) - q_k(N-1) \quad (10)$$

$$\Delta f_k(\mathrm{r}) = f_k^+ - f_k^- \quad (11)$$

f_k^+ and f_k^- are Fukui functions for nucleophilic and electrophilic attacks, respectively, $q_k(N+1)$, $q_k(N)$ and $q_k(N-1)$ are the electron population of atom k in the cationic, neutral, and anionic forms. $\Delta f_k(\mathrm{r})$ is the dual descriptor that allows for unambiguous identification reactivity sites.

Figure-2. Optimized structure of the investigated molecules

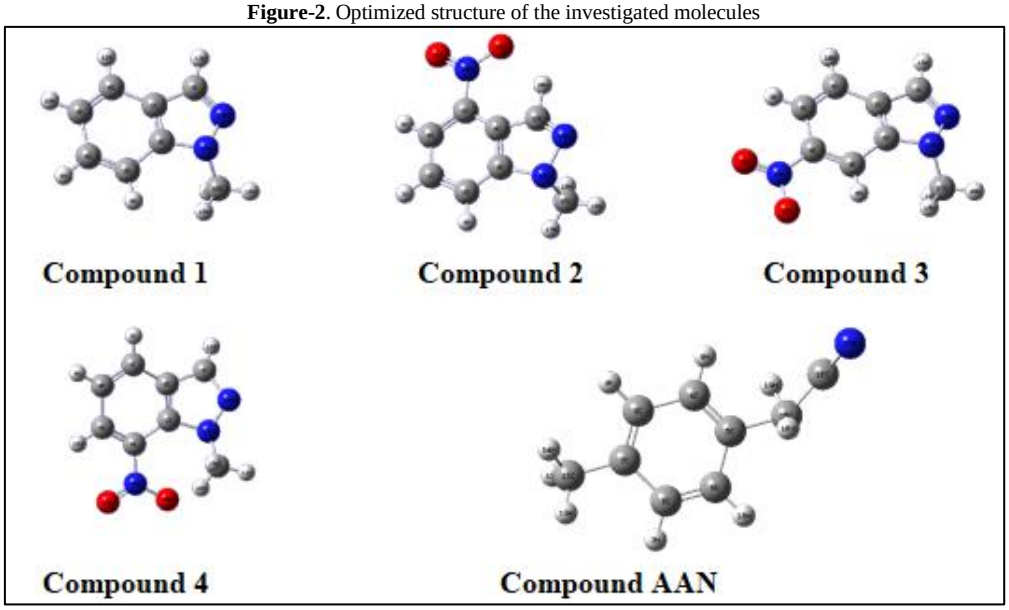

3. Results and Discussion

3.1. NMR Analysis

NMR data will be analysed and interpreted on the basis of nitro group and the local effects recorded on each atom position.

3.1.1. ^{13}C-NMR Analysis

^{13}C-NMR data presented in Table 1 give a general overview of chemical shifts from 1-methyl-indazole, 1-methyl-4-nitro-indazole, 1-methyl-6-nitro-indazole and 1-methyl-7-nitro-indazole (4) evolution. As for the values in brackets indicated in Table 1, they permit to clarify the differences in chemical shifts between the data for 1-methyl-indazole and its nitro derivatives which relate to compounds 2, 3 and 4.

The substitution of 1-methy-Indazole with a nitro group produces the following general trends: the largest effect is observed, as expected, on the chemical shifts of the signals of the carbon atoms directly bound to the nitro group which move towards the weak fields, from about 20 to 26 ppm. This effect is quite similar to that already observed for nitrobenzene (Δδ = +20.0 ppm compared to benzene), for 1-nitro- and 2-nitronaphthalene (Δδ= +19.0 and +19.8 ppm compared to naphthalene) [27].

The substitution of 1-methy-Indazole with a nitro group produces the following general trends: the largest effect is observed, as expected, on the chemical shifts of the signals of the carbon atoms directly bound to the nitro group which move towards the weak fields, from about 20 to 26 ppm. This effect is quite similar to that already observed for nitrobenzene (Δδ = +20.0 ppm compared to benzene), for 1-nitro- and 2-nitronaphthalene (Δδ= +19.0 and +19.8 ppm compared to naphthalene) [27].

In addition, the resonances of C-3a and C-7a gradually shift towards the weak fields, away from the nitro group. With regard to the preferred "para" positions, in contrast to compounds 3 (C-7a), the effects at the C-7 and C-4 positions, for molecules 2 and 4 respectively, are in perfect agreement with the behaviour observed in parallel for nitrobenzene and 1-nitronaphthalene [28]. This situation indicates that the localisation of the positive charge is not favoured on the junctional carbon atoms.

As far as the effects on the "ortho" positions are concerned, the observed trends are in agreement with the localisation of the positive charge in the corresponding resonance structures. In fact, the ortho effects exhibited by compounds 2 and 4 resemble those reported for nitrobenzene and 1-nitronaphthalene on the one hand and those of compound 3 at 2-nitronaphthalene on the other. In line with the data reported for nitrobenzene and 1-

nitronaphthalene, the preferred "meta" positions in compounds 2 and 4 (C-6 and C-5, respectively) are very weakly influenced by the nitro substituent, reproducing the same situation observed for nitrobenzene and 1-nitronaphthalene.

Table-1. ^{13}C NMR data of 1-methyl-Indazole, 1-methyl-4-, 6- and 7-NitroIndazoles in $CDCl_3$

Compounds	C-3	C-3a	C-4	C-5	C-6	C-7	C-7a	N-CH_3
1-Methyl-Indazole (Compound 1)	132.4	123.8	120.8	120.2	125.9	108.6	139.7	35.2
1-Methyl-4-NitroIndazole (Compound 2)	132.4	116.9	140.6	118.0	125.3	116.0	141.4	36.0
	(0)	(-6.9)	(+19.8)	(-2.2)	(-0.6)	(+7.4)	(+1.7)	(+0.8)
1-Methyl-6-NitroIndazole (Compound 3)	133.1	127.0	121.7	115.2	146.4	105.7	138.5	36.0
	(+0.7)	(+3.2)	(+0.9)	(-5.0)	(+20.5)	(-2.9)	(-1.2)	(+0.8)
1-Methyl-7-NitroIndazole (Compound 4)	134.0	128.9	127.9	119.7	124.6	135.1	131.1	40.9
	(+1.6)	(+5.1)	(+7.1)	(-0.5)	(-1.3)	(+26.5)	(-8.6)	(+5.7)

3.1.2. ^{1}H-NMR Analysis

^{1}H NMR data in $CDCl_3$ of indazole (1), and all these nitro derivatives are reported in Table 2.

Table-2. 1-Methyl-Indazole, 1-methyl-4-, 6- and 7-NitroIndazoles ^{1}H NMR data in $CDCL_3$

Compounds	H-3	H-4	H-5	H-6	H-7	N-CH_3
1-Méthyl-Indazole (Compound 1)	8.14	7.79	7.19	7.40	7.52	3.85
1-Méthyl-4-NitroIndazole (Compound 2)	8.60		8.10	7.49	7.75	4.16
	(+0.46)	()	(+0.91)	(+0.09)	(+0.23)	(+0.31)
1-Méthyl-6-NitroIndazole (Compound 3)	8.08	7.81	7.98		8.36	4.17
	(-0.06)	(+0.02)	(+0.79)	()	(0.84)	(+0.32)
1-Méthyl-7-NitroIndazole (Compound 4)	8.13	8.01	7.21	8.10		4.24
	(-0.01)	(+0.22)	(+0.02)	(+0.70)	()	(+0.39)

Comparison of the chemical shifts of the H-3 proton of 1-methyl-indazole and 1-methyl-4, 6 and 7-nitro-indazoles shows that the electron attraction effect of the nitro group on the indazole ring results in a shift of the H-3 proton resonance of 1-Methyl-4-NitroIndazole (2) towards the weak fields. For compounds 3 and 4, the H-3 resonances undergo a small shift towards the strong fields as the nitro group moves away from the H-3 proton.

Regarding the effects on the "ortho" preferential positions, the presence of the nitro group at position 6 results in a significant shift towards the weak fields for H-5 (by 0.79 ppm) and H-7 (by 0.84 ppm). This observation would mean that the H-7 proton is much more unlocked than that at position 5. A similar behaviour is observed for the signals of the H-5 and H-6 protons, respectively for the 4- and 7-nitroindazole derivatives.

Furthermore, the protons belonging to the benzene ring in the "meta" position of the nitro group appear at weaker magnetic fields than the others (H-6 for the 4-nitro derivative, H-4 for the 6-nitro derivative and H-5 for the 7-nitro derivative). This was to be expected given the weak influence of the electronic effects of the nitro group on these positions.

3.2. DFT Examination

3.2.1. Global Reactivity Investigation

Global chemical parameters values were calculated at B3LYP/6-311G (d, p) are recorded in Table 3.

Table-3. Global quantum chemical parameters at B3LYP/6-311G (d, p)

Parameters	Compound 1	Compound 2	Compound 3	Compound 4	AAN
E_{HOMO} (eV)	-6.0229	-6.7589	-6.7165	-6.7189	-6.8851
E_{LUMO} (eV)	-0.9466	-2.7676	-2.6738	-2.6827	-0.6593
ΔE (eV)	5.0763	3.9913	4.0427	4.0362	6.2258
μ (D)	2.2045	6.0051	3.8507	5.0738	6.0503
I (eV)	6.0229	6.7589	6.7165	6.7189	6.8851
A (eV)	0.9466	2.7676	2.6738	2.6827	0.6593
χ (eV)	3.4848	4.7633	4.6952	4.7008	3.7722
η (eV)	2.5382	1.9957	2.0214	2.0181	3.1129
σ $(eV)^{-1}$	0.3940	0.5010	0.4947	0.4955	0.3212
ω	2.3923	5.6846	5.4530	5.4748	2.2856
E_T (Ha)	-419.2597	-623.7665	-623.8164	-623.8089	-403.2219
CPU	1h30mn42s	8h20mn33s	2h17mn23s	5h21mn46s	3h13min7.0s

An organic compound reactivity depends on its ability to donate or accept electrons. The parameters that express electron donation and acceptance are HOMO and LUMO orbitals energies, respectively [29, 30]. Indeed, according to values obtained in literature [31, 32], it was found that E_{HOMO} values of studied molecules are high, suggesting that they can react by donating electrons to an electron acceptor. These values are in is the trend: E_{HOMO} (1)>E_{HOMO} (3)>E_{HOMO} (4) >E_{HOMO}(2) > E_{HOMO}(AAN), certifying that compound 1 has the best electron donating ability. While the low values of E_{LUMO} obtained with the studied compounds, relate that these molecules are likely to accept electrons from another compound. HOMO and LUMO orbitals are linked to charge transfer and charge acceptance respectively [31, 32]. Frontier molecular orbital (FMO) theory, which consists of the most occupied molecular orbital (HOMO) and the least occupied molecular orbital (LUMO), gives an estimate of how electrons interact with the different orbitals, leading to the electronic distribution within each molecule. Figure 3 shows this distribution for each molecule under consideration.

Regarding the energy gap (ΔE), this parameter permits to prove the reactivity of an organic molecule and its ability to react with other compounds. The energy gap is a parameter that describes the chemical reactivity of an organic compound. The molecular energy gap between HOMO and LUMO orbitals, called ΔE, is used to judge the molecular electron-donating and electron-receiving capacity [33, 34]. A low value of ΔE indicates that the molecule's electron-donating capacity is stronger, so it reacts more readily with other molecules to give other stable compounds. ΔE values obtained with the studied molecules are low and are in the following order: ΔE (2) < ΔE (4) < ΔE (3) < ΔE (1) < ΔE (AAN), therefore they have a good ability to react easily with other molecules. It is found that compound 2 has a good reactivity than the other compounds, while the compound AAN is the least reactive.

The three compounds 2, 4 and 3 which have NO_2 in their structure are more reactive than compounds 1 and AAN which do not have NO_2 in its structure. The low reactivity of AAN could be influenced by the attacking group CN. It appears in this case that the NO_2 substituent would reinforce the chemical reactivity of these three compounds.

The ionization energy (*I*) and the electron affinity (*A*) of a compound relate its predisposition to give or receive electrons [32]. The low values of *I* and the high values of *A* displayed in the table confirm these properties of giving and accepting electrons.

Furthermore, the studied compounds possess low values of global hardness(η) and high values of global softness (σ). According to the literature, these values offer low resistance to the molecules during charge transfer; thus, these studied compounds have good chemical reactivity [35]. In this study, the high values of ω attests that these molecules could be good electrophiles [36]. Therefore they possess a good ability to accept electrons from another compound. The negative values of the total energy indicate that the electron transfers are very favorable [37].

Figure-3. LUMO and HOMO distribution of different molecules studied.

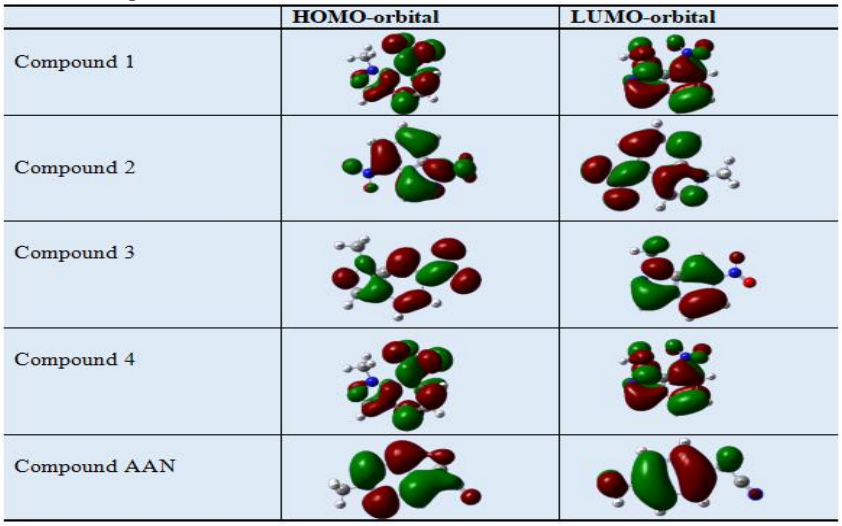

3.2.2. Local Reactivity Investigation

Local parameters calculated through Fukui functions and dual descriptor for different molecules are listed in the tables below.

Table-4. Mulliken atomic charges, Fukui functions and dual descriptor of compound 1

Atoms	$q_k(N+1)$	$q_k(N)$	$q_k(N-1)$	f_k^+	f_k^-	$\Delta f_k(\mathbf{r})$
1 C	-0.048103	-0.222354	0.021393	0.174251	-0.243747	0.417998
2 C	-0.083358	0.212029	-0.056982	-0.295387	**0.269011**	**-0.564398**
3 C	0.285831	-0.073408	0.237008	0.359239	-0.310416	0.669655
4 C	-0.052738	-0.103767	0.204348	0.051029	-0.308115	0.359144
5 C	0.151866	-0.109204	-0.080882	0.26107	-0.028322	0.289392
6 C	0.189383	-0.070691	0.345166	0.260074	-0.415857	0.675931
7 C	0.288501	0.120252	0.058456	0.168249	0.061796	0.106453
8 H	-0.014009	0.107515	-0.01669	-0.121524	0.124205	-0.245729
9 H	0.001259	0.108432	-0.014383	-0.107173	0.122815	-0.229988
10 H	-0.008582	0.105855	0.00292	-0.114437	0.102935	-0.217372
11 H	-0.008804	0.100836	-0.021988	-0.10964	0.122824	-0.232464
12 H	-0.014149	0.11473	-0.005259	-0.128879	0.119989	-0.248868
13 N	-0.086348	-0.198396	0.288467	0.112048	-0.486863	0.598911
14 N	0.370495	-0.28927	0.028006	**0.659765**	-0.317276	**0.977041**
15 C	-0.021479	-0.168681	-0.004558	0.147202	-0.164123	0.311325
16 H	0.024818	0.117073	0.00811	-0.092255	0.108963	-0.201218
17 H	0.024804	0.117777	0.008105	-0.092973	0.109672	-0.202645
18 H	0.000611	0.131273	-0.001237	-0.130662	0.13251	-0.263172

Table-5. Mulliken atomic charges, Fukui functions and dual descriptor of compound 2

Atoms	$q_k(N+1)$	$q_k(N)$	$q_k(N-1)$	f_k^+	f_k^-	$\Delta f_k(\mathbf{r})$
1 C	-0.024704	-0.084289	-0.036275	0.059585	-0.048014	0.107599
2 C	0.233014	-0.037607	0.22406	0.270621	-0.261667	0.532288
3 C	-0.078935	0.12223	-0.055475	-0.201165	**0.177705**	**-0.37887**
4 C	-0.032064	-0.064036	0.072235	0.031972	-0.136271	0.168243
5 C	0.17188	0.18863	0.070013	-0.01675	0.118617	-0.135367
6 C	0.084985	-0.040978	0.125547	0.125963	-0.166525	0.292488
7 H	0.000215	0.125198	0.000889	-0.124983	0.124309	-0.249292
8 H	-0.011339	0.119185	-0.014029	-0.130524	0.133214	-0.263738
9 H	-0.005609	0.138891	-0.00796	-0.1445	0.146851	-0.291351
10 N	-0.022861	0.10213	0.173279	-0.124991	-0.071149	-0.053842
11 O	0.173729	-0.200854	0.176832	0.374583	-0.377686	0.752269
12 O	-0.117544	-0.305544	0.170492	0.188	-0.476036	0.664036
13 C	0.318598	0.094949	-0.030046	0.223649	0.124995	0.098654
14 N	-0.092975	-0.124558	0.124134	0.031583	-0.248692	0.280275
15 N	0.386048	-0.337061	0.00564	**0.723109**	-0.342701	**1.06581**
16 C	-0.020875	-0.165809	-0.001072	0.144934	-0.164737	0.309671
17 H	0.026426	0.119318	0.000904	-0.092892	0.118414	-0.211306
18 H	0.000548	0.13877	-0.000401	-0.138222	0.139171	-0.277393
19 H	0.026396	0.102799	0.000904	-0.076403	0.101895	-0.178298
20 H	-0.014932	0.108636	0.00033	-0.123568	0.108306	-0.231874

Table-6. Mulliken atomic charges, Fukui functions and dual descriptor of compound 3

Atoms	$q_k(N+1)$	$q_k(N)$	$q_k(N-1)$	f_k^+	f_k^-	$\Delta f_k(\mathbf{r})$
1 C	-0.043388	-0.216226	0.093378	0.172838	-0.309604	0.482442
2 C	-0.082555	0.205994	-0.051553	-0.288549	**0.257547**	**-0.546096**
3 C	0.245177	-0.011031	0.22748	0.256208	-0.238511	0.494719
4 C	-0.045939	0.140306	0.053673	-0.186245	0.086633	-0.272878
5 C	0.164912	-0.072436	0.004083	0.237348	-0.076519	0.313867
6 C	0.172124	-0.058731	0.016509	0.230855	-0.07524	0.306095
7 C	0.306828	0.132296	-0.050072	0.174532	0.182368	-0.007836
8 H	-0.011755	0.148901	-0.013705	-0.160656	0.162606	-0.323262
9 H	-0.008311	0.138027	-0.001435	-0.146338	0.139462	-0.2858
10 H	-0.008176	0.115949	-0.001136	-0.124125	0.117085	-0.24121
11 H	-0.014918	0.124629	0.001881	-0.139547	0.122748	-0.262295
12 N	0.378703	-0.286125	0.035691	**0.664828**	-0.321816	**0.986644**

13 N	-0.092745	-0.182321	0.140933	0.089576	-0.323254	0.41283
14 N	0.000598	0.136183	0.186878	-0.135585	-0.050695	-0.08489
15 O	-0.050138	-0.212416	0.196263	0.162278	-0.408679	0.570957
16 O	0.05762	-0.319549	0.157747	0.377169	-0.477296	0.854465
17 C	-0.020141	-0.173773	-0.003661	0.153632	-0.170112	0.323744
18 H	0.025807	0.126732	0.00371	-0.100925	0.123022	-0.223947
19 H	0.02577	0.124174	0.003706	-0.098404	0.120468	-0.218872
20 H	0.000527	0.139417	-0.000372	-0.13889	0.139789	-0.278679

Table-7. Mulliken atomic charges, Fukui functions and dual descriptor of compound 4

Atoms	$q_k(N+1)$	$q_k(N)$	$q_k(N-1)$	f_k^+	f_k^-	$\Delta f_k(\mathrm{r})$
1 C	-0.09604	0.205182	0.033153	-0.301222	**0.172029**	**-0.473251**
2 C	-0.016447	-0.150689	-0.034192	0.134242	-0.116497	0.250739
3 C	0.119696	-0.051786	0.263779	0.171482	-0.315565	0.487047
4 C	0.179023	-0.104214	-0.088463	0.283237	-0.015751	0.298988
5 C	-0.086059	-0.052808	0.209205	-0.033251	-0.262013	0.228762
6 C	0.263899	0.2081	0.017593	0.055799	0.190507	-0.134708
7 C	0.280352	0.042013	0.036325	0.238339	0.005688	0.232651
8 H	-0.005525	0.120947	-0.016246	-0.126472	0.137193	-0.263665
9 H	-0.009538	0.124693	0.003742	-0.134231	0.120951	-0.255182
10 H	0.002789	0.144795	-0.01194	-0.142006	0.156735	-0.298741
11 H	-0.013733	0.140179	-0.002265	-0.153912	0.142444	-0.296356
12 N	-0.089737	-0.163481	0.043378	0.073744	-0.206859	0.280603
13 N	0.386231	-0.27015	-0.021524	**0.656381**	-0.248626	**0.905007**
14 C	-0.01462	-0.24021	0.000996	0.22559	-0.241206	0.466796
15 H	0.024052	0.103671	-0.0007	-0.079619	0.104371	-0.18399
16 H	0.029305	0.164215	-0.000998	-0.13491	0.165213	-0.300123
17 H	0.000719	0.118216	-0.000299	-0.117497	0.118515	-0.236012
18 N	-0.030309	0.13167	0.210309	-0.161979	-0.078639	-0.08334
19 O	0.063217	-0.204618	0.175505	0.267835	-0.380123	0.647958
20 O	0.012725	-0.315725	0.182624	0.32845	-0.498349	0.826799

Table-8. Mulliken atomic charges, Fukui functions and dual descriptor of AAN

Atoms	$q_k(N+1)$	$q_k(N)$	$q_k(N-1)$	f_k^+	f_k^-	$\Delta f_k(\mathrm{r})$
1 C	-0.02176	-0.068797	0.071414	0.047037	-0.140211	0.187248
2 C	0.123136	-0.112877	-0.018798	0.236013	-0.094079	0.330092
3 C	0.002841	-0.070779	0.022804	0.07362	-0.093583	0.167203
4 C	0.086526	-0.096553	0.038961	0.183079	-0.135514	0.318593
5 C	0.037264	-0.151412	0.201901	0.188676	-0.353313	0.541989
6 C	0.030812	-0.034561	-0.014856	0.065373	-0.019705	0.085078
7 H	0.001017	0.108929	0.002946	-0.107912	0.105983	-0.213895
8 H	0.000846	0.104546	0.001683	-0.1037	0.102863	-0.206563
9 H	-0.004716	0.110712	0.008311	-0.115428	0.102401	-0.217829
10 H	-0.000807	0.110815	0.009971	-0.111622	0.100844	-0.212466
11 C	-0.005765	-0.25476	0.00137	0.248995	-0.25613	0.505125
12 H	-0.003324	-0.044536	0.22002	-0.458788	-0.264556	-0.194232
13 H	0.003329	0.116856	-0.000511	-0.113527	0.117367	-0.230894
14 H	0.001891	0.118857	0.000261	-0.116966	0.118596	-0.235562
15 C	0.674815	-0.275283	-0.113504	**0.950098**	-0.161779	**1.111877**
16 C	0.008681	0.134789	0.000037	-0.126108	**0.134752**	**-0.26086**
17 N	0.186319	-0.237097	-0.026295	0.423416	-0.210802	0.634218
18 H	-0.006016	0.254448	0.263415	-0.260464	-0.008967	-0.251497
19 H	-0.01509	0.252704	0.330872	-0.267794	-0.078168	-0.189626

Probable reactivity sites for nucleophilic attacks identification are located by the highest values of f_k^+ and $\Delta f_k(\mathrm{r})$. Whereas the probable reactivity site for nucleophilic attacks is identified by the highest value of f_k^- and the lowest value of $\Delta f_k(\mathrm{r})$. These sites constitute electronic exchange center where the molecule can lose or gain electrons. Table 9 summarizes the various probable attack sites for each compound studied.

Table-9. Different reactivity sites for the compounds studied

Compound	Nucleophilic attack site	Electrophilic attack site
1	14N	2C
2	15N	3C
3	12N	2C
4	13N	1C
AAN	15C	16C

3.3. Reactivity between Compounds 2 to 4 and 2-(p-tolyl) Acetonitrile

The scheme 1 below gives a general overview of the reactivities between compounds 2 to 4 and 2-(p-tolyl)acetonitrile.

Scheme-1. Nucleophilic substitution reaction between studied alkyl nitroindazole and aryl acetonitrile

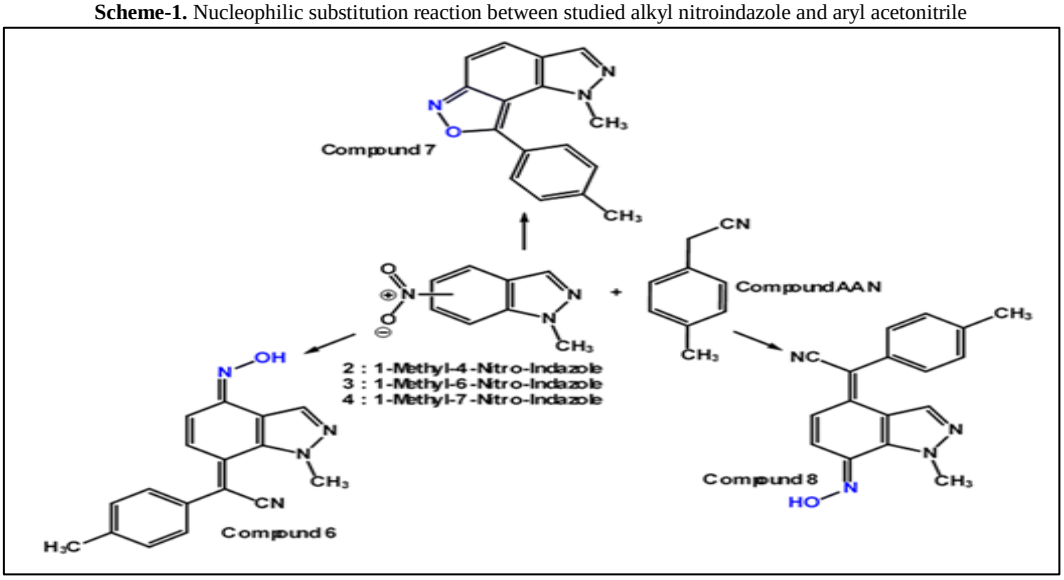

In order to explain compound 6 formation, we proposed the following mechanism (Scheme 2): the initial step of the reaction corresponds to the formation of intermediate A, via the attack of the carbanion of 2-(p-tolyl)acetonitrile in position 7 of indazole. The rearrangement of A followed by the elimination of a water molecule leads to the intermediate B. The latter undergoes tautomerism to lead to compound 6.

Scheme-2. Proposed reaction mechanism for the formation of compound 6

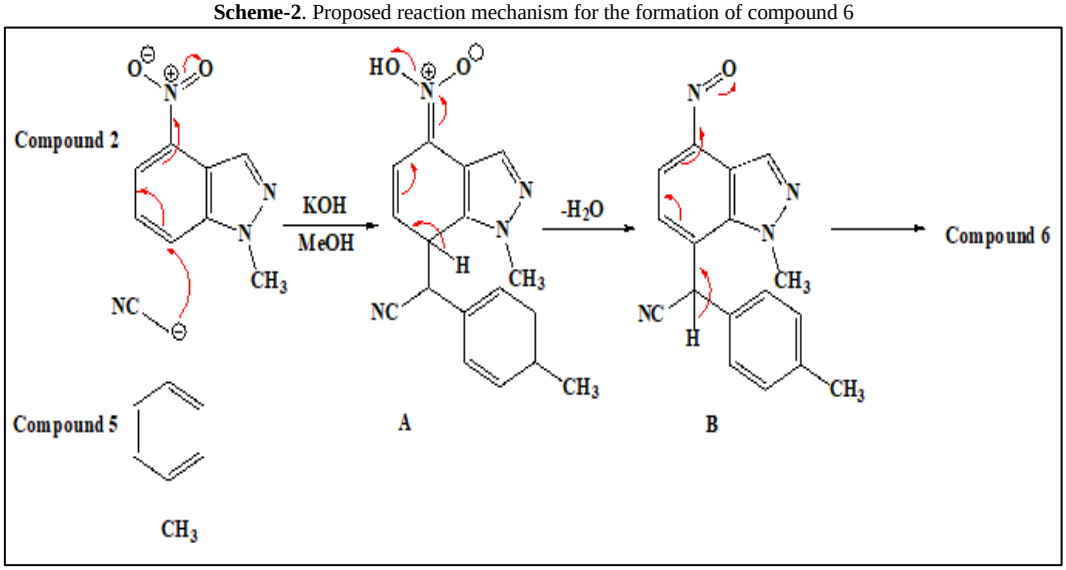

The mechanism formation of compound 8 is similar to that presented in Scheme 2. The aromatic nucleophilic substitution of 2-(p-tolyl)acetonitrile occurs at the para position (C-4) relative to the nitro group of 1-methyl-7-nitroindazole, the reaction is regioselective.

In order to explain the formation of the isoxazolo[3,4-g]indazole ring (compound 7), we proposed the following mechanism: the first step corresponds to the attack of the carbanion of arylacetonitrile at the 'ortho' position (carbon 7) of the nitro group, followed by tautomerism leading to the intermediate B. Intramolecular cyclization of B, followed by aromatization of the isoxazole ring, with removal of CN at C, leads to the compound 7 (Scheme 3).

Scheme-3. Proposed reaction mechanism for the formation of compound 7

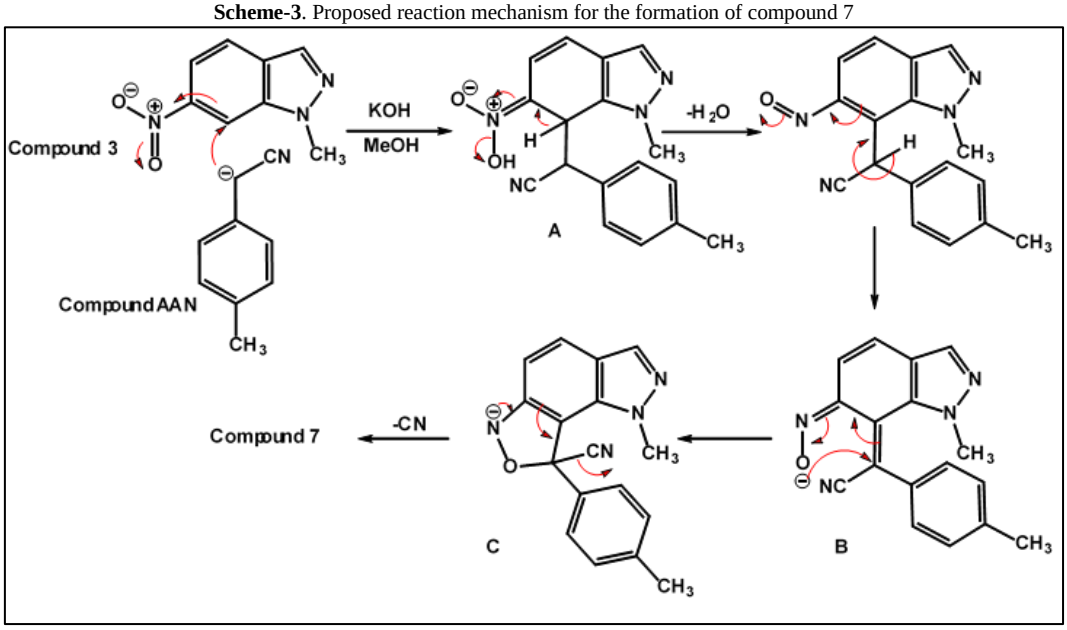

These original results clearly demonstrate the importance of the position of the nitro group of the indazole benzene homocycle in the regioselectivity of the nucleophilic substitution reaction of arylacetonitriles within 1-alkyl-nitroindazoles.

3.4. Correlation between NMR and DFT Data

The reactivity parameters of compounds 1,2,3,4 and AAN clearly show that these compounds are highly reactive. This reactivity is due to their ability to donate and receive electrons. This electron mobility is confirmed by the ^{1}H-NMR and ^{13}C-NMR chemical shifts of the different species within each compound, as reported by the experimental NMR approach. These different shifts highlight the mechanism of formation of the compounds obtained in Schemes 1, 2 and 3. These findings demonstrate that DFT approach is closely linked to the NMR data. Similar results were obtained in the literature [38, 39].

4. Conclusion

The results of this work allow us to draw the following conclusions:

- Theoretical data based on DFT indicate that the studied compounds possess good reactivity;
- ^{13}C-NMR and ^{1}H-NMR analysis shows that the position of ortho, para and metal groups are generally influenced by the nitro group;
- Nucleophilic and electrophilic reactivity of the studied compounds revealed the active sites within each compound;
- Formation of nitro compounds mechanism has been established, clearly explaining the various stages of formation;
- There is good correlation between data from DFT calculations and experimental ^{1}H and ^{13}C NMR.

References

[1] Cerecetto, H., Gerpe, A., Gonzalez, M., Aran, V. J., and deOcariz, C. O., 2005. "Pharmacological properties of indazole derivatives: Recent developments." *Mini Reviews in Medicinal Chemistry*, vol. 5, pp. 869–878.

[2] Jennings, A. and Tennant, M., 2007. "Selection of molecules based on shape and electrostatic similarity: Proof of concept of “electroforms." *Journal of Chemical Information and Modeling*, vol. 47, pp. 1829–1838.

[3] Han, W., Pelletier, J. C., and Hodge, C. N., 1998. "Hodge, Tricyclic ureas: A new class of HIV-1 protease inhibitors." *Bioorganic and Medicinal Chemistry Letters*, vol. 8, pp. 3615–3620.

[4] Rosati, O., Curini, M., Marcotullio, M. C., Macchiarulo, A., Perfumi, M., Mattioli, L., Rismondo, F., and Cravotto, G., 2007. "Synthesis, docking studies and anti-inflammatory activity of 4,5,6,7-tetrahydro-2H-indazole derivatives." *Bioorganic and Medicinal Chemistry*, vol. 15, pp. 3463–3473.

[5] Li, X., Chu, S., Feher, V. A., Khalili, M., Nie, Z., Margosiak, S., Nikulin, V., Levin, J., Sprankle, K. G., *et al.*, 2003. "Structure-based design, synthesis, and antimicrobial activity of indazole-derived sah/mta nucleosidase inhibitors." *Journal ofMedicinal Chemistry*, vol. 46, pp. 5663–5673.

[6] Takahashi, H., Shinoyama, M., Komine, T., Nagao, M., Suzuki, M., Tsuchida, H., and Katsuyama, K., 2011. "Novel dihydrothieno[2,3-e]indazole derivatives as IκB kinase inhibitors." *Bioorganic and Medicinal Chemistry Letters*, vol. 21, pp. 1758–1762.

[7] Lee, F. Y., Lien, J. C., Huang, L. J., Huang, T. M., Tsai, S. C., Teng, C. M., Wu, C. C., Cheng, F. C., and Kuo, S. C., 2011. "Synthesis of 1-benzyl-3-(5‘-hydroxymethyl-2‘-furyl)indazole analogues as novel antiplatelet agents." *Journal of Medicinal Chemistry*, vol. 44, pp. 3746–3749.

[8] Chen, C. J., Hsu, M. H., Huang, L. J., Yamori, T., Chung, F. G., Lee, F. Y., Teng, C. M., and Kuo, S. C., 2008. "Anticancer mechanisms of YC-1 in human lung cancer cell line, NCI-H226." *Biochemical Pharmacology*, vol. 75, pp. 360–368.

[9] Bouchet, P., Lazaro, R., Benchidmi, M., and J., E., 1980. "Photochimie d'heterocycles azotes—VI: Synthese par voie photochimique d'amino et d'alkoxy indazoles." *Tetrahedron*, vol. 36, pp. 3523-3533.

[10] Boga, C., Calvaresi, M., Franchi, P., Lucarini, M., Fazzini, S., Spinelli, D., and Tonelli, D., 2012. "Electron reduction processes of nitrothiophenes. A systematic approach by DFT computations, cyclic voltammetry and E-ESR spectroscopy." *Organic Biomolecular Chemistry*, vol. 10, pp. 7986-7995.

[11] Kouakou, A., Gabriele, M., Carla, B., Matteo, C., Hakima, C., Paola, F., Lorella, G. L., Marco, E. M., Rakib, *et al.*, 2015. "Spectroscopic and electrochemical properties of 1- or 2-alkyl substituted 5- and 6-nitroindazoles. Spectroscopic and Electrochemical Properties of 1- or 2-alkyl Substituted 5- and 6-Nitroindazoles." *Current Organic Chemistry*, vol. 19, pp. 1526-1537.

[12] Laghchioua, F. E., Kouakou, A., Eddahmi, M., Viale, M., Monticone, M., Gangemi, R., Maric, I., El Ammari, L., Saadi, M., *et al.*, 2020. "Antiproliferative and apoptotic activity of new indazole derivatives as potential anticancer agents." *Archiv pharma Chemistry in life Science*, vol. 353, p. 2000173.

[13] Dhaifallah, M. A., Abdulrahman, I. A., Natarajan, A., Sevgi, K., Necmi, D., Saied, M. S., Mohammad, A., and Raju, S. K., 2020. "Highly functionalized N-1-(2-pyridinylmethyl)-3,5-bis[(E)-arylmethylidene]tetrahydro-4(1H)-pyridinones:Synthesis, characterization, crystal structure and DFT studies." *Journal of Molecular Structure*, vol. 1222, p. 128940.

[14] Ansari, K. R., Singh, A., Ismat, H. A., EL Ibrahimi, B., Raj, Sharma, N., Bansal, A., Abdullah, K. A., Muhammad, Y., *et al.*, 2023. "Hetroatomic organic compound as a novel corrosion inhibitor for carbon steel in sulfuric acid: Detail experimental, surface, molecular docking and computational studies." *Colloids and Surfaces A: Physicochemical and Engineering Aspects*, vol. 640, p. 131692.

[15] Zhang, Q. H., Xu, N., Jiang, Z. N., Liu, H. F., and Zhang, G. A., 2023. "Chitosan derivatives as promising green corrosion inhibitors for carbon steel in acidic environment: Inhibition performance and interfacial adsorption mechanism." *Journal of Colloid and Interface Science*, vol. 640, pp. 1052-1067.

[16] Albayati, M. R., Kansız, S., Dege, N., Savaş, K., Marzouki, R., Lgaz, H., and Chung Ill., M., 2020. "Synthesis, crystal structure, Hirshfeld surface analysis and DFT calculations of 2-[(2,3-dimethylphenyl)amino]-N'-[(E)-thiophen-2-ylmethylidene]benzohydrazide." *Journal of Molecular Structure*, vol. 1205, p. 127654.

[17] Ambrish, S., Ansari, K. R., Ismat, H. A., Yuanhua, L., and Brahim, E. I., 2022. "Combination of experimental, surface and computational insight into the corrosion inhibition of pyrimidine derivative onto Q235 steel in oilfield acidizing fluid under hydrodynamic condition." *Journal of Molecular Liquids*, vol. 3.53, p. 118825.

[18] Bahlakeh, G., Ramezanzadeh, B., Dehghani, A., and Ramezanzadeh, M., 2019. "Novel cost-effectiveand high-performance green inhibitor based on aqueous Peganum harmala seed extract for mild steel corrosion in HCl solution: detailed experimental and electronic/atomic level computational explorations." *Journal of Molecular Liquids*, vol. 283, pp. 174-195.

[19] Frisch, M. J., Trucks, G. W., Schlegel, H. B., Scuseria, G. E., Robb, M. A., and Cheeseman, J. R., 2009. *Fox. Gaussian*. Gaussian, Inc., Wallingford CT, p. 9.

[20] Becke, D., 1986. "Density functional calculations of molecular bond energies." *The Journal of Chemical Physics*, vol. 84, pp. 4524-4529.

[21] Lee, C., Yang, W., and Parr, R. G., 1988. "Development of the colle-salvetti correlation-energy formula into a functional of the electron density." *Physical Review B.*, vol. 37, pp. 785-789.

[22] Allal, H., Belhocine, Y., and Zouaoui, E., 2018. "Computational study of some thiophene derivatives as aluminium corrosion inhibitors." *Journal of Molecular Liquids*, vol. 265, pp. 668–678.

[23] Damej, M., Benmessaoud, M., Zehra, S., Kaya, S., Hassane, L., Molhi, A., Labjar, N., El Hajjaji, S., Awad, A. A., *et al.*, 2021. "Experimental and theoretical explorations of S-alkylated mercaptobenzimidazole derivatives for use as corrosion inhibitors for carbon steel in HCl." *Journal of Molecular Liquids*, vol. 331, p. 115708.

[24] Chaouiki, A., Lgaz, H., Chung, I. M., Ali, I. H., Gaonkar, S. L., Bhat, K. S., Salghi, R., Oudda, H., and Khan, M. I., 2018. "Understanding corrosion inhibition of mild steel in acid medium by new benzonitriles: insights from experimental and computational studies." *Journal of Molecular Liquids*, vol. 266, pp. 603–616.

[25] Martinez-Araya, J. I., 2015. "Why is the dual descriptor a more accurate local reactivity descriptor than fukui functions." *Journal of Mathematical Chemistry*, vol. 5, pp. 451-465.

[26] Morell, C., Grand, A., and Toro-Labbé, A., 2005. "New dual descriptor for chemical reactivity." *Journal of Physical Chemistry A*, vol. 109, pp. 205-212.

[27] Ernst, L., 1976. "13C NMR spectroscopy of polycyclic aromatics VII. Naphthalenes carrying electron-withdrawing substituents. Correlations between substituent- induced shifts and INDO MO charge densities." *Journal of Magnetic Resonance*, vol. 22, pp. 279-287.

[28] Wehrli, F. W. and Wirthlin, T. *Interpretation of carbon-13 nmr spectra*. London: Heyden. p. 1978.

[29] Heba, E. H., Ahmed, A. F., Eslam, A. M., and Eman, M. A., 2022. "Experimental and theoretical assessment of benzopyran compounds as inhibitors to steel corrosion in aggressive acid solution." *Journal of Molecular Structure*, vol. 1249, p. 131641.

[30] Khattabi, M., Benhiba, F., Tabti, S., Djedouani, A., El Assyry, A., Touzani, R., Warad, I., Oudda, H., and Zarrouk, 2019. "Performance and computational studies of two soluble pyran derivatives as corrosion inhibitors for mild steel in HCl." *Journal of Molecular Structure,* vol. 1196, pp. 231-244.

[31] Abdallah, E. A., Aaziz, J., Moutie, M. R., Rachid, O., Khalid, A., Hanane, Z., Mustapha, H., Hassan, B., Lahcen, B., *et al.*, 2022. "Computational and experimental studies of the inhibitory effect of imidazole derivatives for the corrosion of copper in an acid medium." *Journal of Molecular Liquids,* vol. 345, p. 117813.

[32] Messali, M., Larouj, M., Lgaz, H., Rezki, N., Al-Blewi, M. F. F., Aouad, M. R. A., Chaouiki, and Salghi, R. I.-M. C., 2018. "A new schiff base derivative as an effective corrosion inhibitor for mild steel in acidic media: Experimental and computer simulations studies." *Journal of Molecular Structure,* vol. 1168, pp. 39-48.

[33] Laadam, G., 2023. "Outstanding anti-corrosion performance of two pyrazole derivatives on carbon steel in acidic medium: Experimental and quantum-chemical examinations." *Journal of Molecular Liquids,* vol. 375, p. 121268.

[34] Singh, A., Ansari, K. R., Kumar, A., Liu, W., Songsong, C., and Liu, Y., 2017. "Electrochemical, surface and quantum chemical studies of novel imidazole derivatives as corrosion inhibitors for J55 steel in sweet corrosive environment." *Journal of Alloys and Compounds,* vol. 712, pp. 121-133.

[35] Hamrahi, B., Khanlarkhani, A., Morteza, M. S., Fattah, a. A., and Gashti, S. O., 2021. "evaluation of henna extract performance on corrosion inhibition of api 5l steel in h2s containing medium and dft quantum computing of its constituents." *Metals and Materials International,* vol. 27, pp. 4463–4476.

[36] Khattabi, M., Benhiba, F., Tabti, S., Djedouani, A., El Assyry, A., Touzani, R., Warad, I., Oudda, H., and Zarrouk, A., 2019. "Performance and computational studies of two soluble pyran derivatives as corrosion inhibitors for mild steel in HCl." *Journal of Molecular Structure,* vol. 1196, pp. 231-244.

[37] Tigori, M. A., Kouyaté, A., Kouakou, V., Niamien, P. M., and Trokourey, A., 2020. "Computational approach for predicting the adsorption properties and inhibition of some antiretroviral drugs on copper corrosion in HNO3." *European Journal of Chemistry,* vol. 11, pp. 235-244.

[38] Konstantinov, I. A. and Broadbelt, L. J., 2011. "Regression formulas for density functional theory calculated 1H and 13C NMR chemical shifs in toluene-d 8." *The Journal of Physical Chemistry A,* vol. 115, pp. 12364–12372.

[39] Pierens, G. K., Venkatachalam, T., and Reutens, D. C., 2016. "Comparison of experimental and DFT-calculated NMR chemical shifs of 2-amino and 2-hydroxyl substituted phenyl benzimidazoles, benzoxazoles and benzothiazoles in four solvents using the IEF-PCM solvation model." *Magnetic Resonance in Chemistry,* vol. 54, pp. 298-307.